Nanosatellite Lasercom System

Rachel Morgan
Massachusetts Institute of Technology
77 Massachusetts Avenue
remorgan@mit.edu

Faculty Advisor: Kerri Cahoy
Massachusetts Institute of Technology

ABSTRACT

The increasing use of CubeSats (small satellites) for scientific and commercial applications has led to a need for reliable, high-rate communications capabilities. Traditional small satellite radio frequency communication systems require large, high gain receive apertures which are limited by the size, weight, and power constraints of CubeSat platforms, and thus make high-rate inter-satellite crosslinks difficult. Optical communications systems can use shorter visible or infrared wavelengths to transmit information at higher data rates with smaller systems. This project focuses on the development, test, and demonstration of an optical transceiver prototype that is compact enough to operate on a CubeSat in order to demonstrate optical crosslinks between small satellites.

INTRODUCTION

Small satellite formations have potential to enable new classes of scientific and commercial missions. These formations can provide near-real-time global coverage at high revisit rates for miniaturized scientific instruments such as multispectral imagers or multi-angle sensor observations, but will require high data rate crosslinks to quickly route data to ground stations. Typical high-rate RF systems (>1 Mbps) for CubeSats rely on relatively large aperture, high-gain ground stations. Large, high-gain apertures or higher power transponders are not feasible on CubeSats due to size, weight, volume, and power constraints, particularly if the CubeSat also must operate its instrument payload at a high duty cycle. Free space laser communication can solve this problem by using shorter visible or infrared wavelengths to transmit information at higher data rates with smaller, more power efficient systems.

We present a design for a monostatic free-space optical transceiver capable of supporting data crosslinks between CubeSats in LEO for the Free Space Lasercom and Radiation Experiment (FLARE). This design includes a detailed link budget analysis and a benchtop prototype to demonstrate the system feasibility. The transceiver module is designed to support a data rate of 20 Mbps at 20-500 km separations using an input power of <20 W and fitting within 1 U (10 cm x 10 cm x 10 cm) of volume. The design consists of an optical assembly to reduce the incoming receive signal and expand the outgoing transmit signal and two microelectromechanical systems (MEMS) Fast Steering Mirrors (FSMs) to improve pointing control and direct the laser signals to the receivers. The system also involves a beam splitter and dichroic filter system to direct the visible calibration beacons to a Quad Cell detector for a feedback loop to control the FSM and send the receive signal to an Avalanche Photodiode Detector to measure the signal. The design also includes a transmitter module consisting of a laser assembly, modulation system, and an Erbium Doped Fiber Amplifier coupled to a collimator to produce a 200 mW signal. The transmitter module has already been designed and prototyped; this paper focuses on creating a combined transceiver assembly and verifying its design. The benchtop prototype is a proof-of-concept setup to demonstrate that the system is operational and will fit within the mission size, weight, and power constraints. The prototype will also be used for testing of the pointing control system. FLARE is being developed as an entry for the Air Force Research Lab's University Nanosatellite Program competition.

Laser communications (lasercom) for space applications has been studied extensively and demonstrated in space by several flight missions on larger spacecraft. Most research in lasercom for CubeSats has focused on CubeSat-to-ground optical links such as MIT's Nanosatellite Optical Downlink Experiment (NODE) 1 and Aerospace Corporation's AeroCube 7 2. These missions are aiming to increase the potential data rates for CubeSat-to-ground links in order to expand the capabilities of small satellites. These missions make use of large ground station telescopes, which would not be able to fit on a CubeSat receiver. A major challenge for FLARE is receiving the

signal with a smaller receive aperture as it is limited by the size constraints of CubeSats.

Optical crosslinks for satellites have been demonstrated by the TESAT Laser Communication Terminal program. This experiment demonstrated bi-directional optical communications crosslinks and high-rate optical downlinks with two satellites in low-earth orbit (LEO). The terminal used for this program had a mass of 35 kg, a volume of .5x.5x.6 m^3 and power draw of 120 W. The satellites achieved 5.6 Gbps data rates at inter-satellite ranges of 1000-5100 km with a telescope diameter of 125 mm 3. The goal of FLARE is to achieve optical crosslinks on a much smaller scale, with a volume of 10x10x10 cm^3 mass of 1 kg, and maximum power draw of 20 W. The mission is designed for 20 Mbps data rate crosslinks at inter-satellite separations of 20-500 km.

High rate crosslinks between small satellites would enable low latency communication capabilities for clusters of small satellites taking multi-angle measurements or global constellations of remote sensing or communications satellites. For instance, clusters of small satellites could use distributed sensors to take multi-angle multi-spectral measurements for earth observation as described by Sreeja Nag 4. This sort of mission would generate large amounts of data that could take advantage of short optical crosslinks to route downlink communications around cloud cover or off-load individual satellite data to a larger satellite to relay to the ground. Another application of crosslinks is for a global constellation of communications satellites. This would require longer crosslinks of 1000-7500 km depending on the density of satellites in the constellation 5. The current FLARE system is not designed for such long link ranges, but the FLARE architecture can be scaled up to meet these longer link requirements.

DESIGN OVERVIEW

The FLARE mission involves two CubeSat satellites (FLARE A and FLARE B) that will perform bi-directional optical communication crosslinks and demonstrate the new Sparrow miniaturized particle spectrometer. Figure 1 shows a drawing of one of the FLARE satellites with the lasercom volume labeled. The design consists of an optical assembly to reduce the incoming receive signal and expand the outgoing transmit signal and two microelectromechanical systems (MEMS) Fast Steering Mirrors (FSMs) to improve pointing control and direct the laser signals to the receivers. The system also incorporates a beam splitter and dichroic filter system to direct the internal calibration beam and incoming beacon signal to a Quad Cell detector for a feedback loop to control the Fast Steering Mirrors and send the receive signal to an Avalanche Photodiode Detector to measure the signal. The design also includes a transmitter module consisting of a laser assembly, modulation system, and an Erbium Doped Fiber Amplifier coupled to a collimator to produce the signal at 200 mW. FLARE A and B will both transmit and receive signals at separated wavelengths with symmetric optical transceiver systems. FLARE A will transmit a 1565 nm signal and receive a 1535 nm signal, while FLARE B will transmit the 1535 nm signal and receive the 1565 nm signal. This wavelength division allows us to filter out the outgoing transmit beam so it doesn't interfere with the detection of the incoming receive signal. This enables potential for full-duplex communications operation.

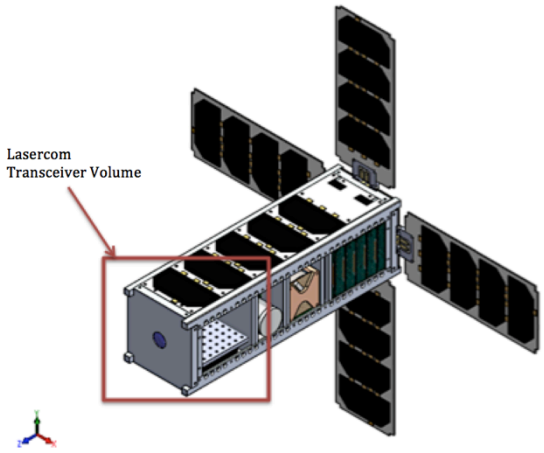

Figure 1: FLARE Satellite Design, image credit: Derek Barnes.

Optical Design

The FLARE optical transceiver is designed to meet the mission requirements of 5 Mbps data rate crosslinks at 25 km link separations, with potential for higher data rates up to 20 Mbps and longer link ranges up to 500 km after the preliminary mission goals have been completed. It is a mono-static design with a shared optical path for the transmit and receive signals. Figure 2 shows a diagram of the optical design for one satellite, with different colors to represent the different wavelengths used throughout the system. The FLARE optical system involves five different laser signals: the transmitted communications signal, the received communications signal, the transmitted beacon signal, the received beacon signal, and the internal calibration signal.

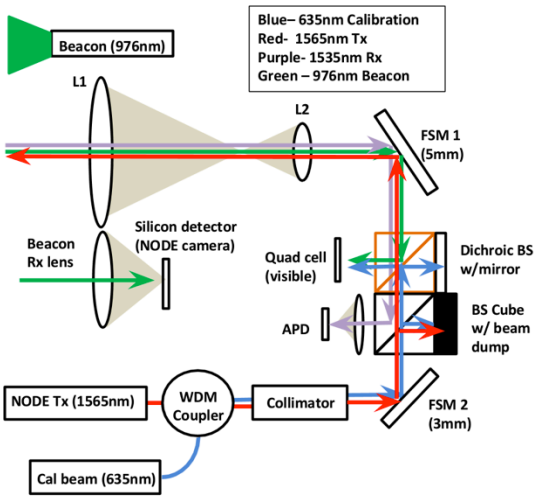

Figure 2: FLARE optical design, image credit: Michael Long.

The transmitted communications signal originates from a transmitter based on the Nanosatellite Optical Downlink Experiment (NODE) design 1. The transmitter contains a low power infrared laser source at either 1565 nm for FLARE A or 1535 nm for FLARE B, which will be modulated using Pulse Position Modulation (PPM). Pulse Position Modulation means that a single laser pulse encoding M bits of information is sent in one of 2^M slots. The square shape of each pulse is generated using a drive current to slightly change wavelength of the laser; the laser light is sent on to a narrow-band Fiber Bragg Grating (FBG) filter. When the laser wavelength is tuned to slightly off of the center wavelength, the Fiber Bragg Grating transmits the light and when the laser is tuned to exactly the center wavelength, the Fiber Bragg Grating reflects it, creating a pulse in a specified slot.

The modulated laser light is then passed through an Erbium Doped Fiber Amplifier (EDFA) that amplifies the optical signal. The signal is combined with the calibration beam using a Wavelength Division Multiplexing (WDM) coupler and then sent through a collimator, which turns the light in the fiber into a collimated free space beam. The signal is then reflected off of a fast steering mirror, passed though the beam splitter/dichroic mirror assembly, reflected off a second Fast Steering Mirror, expanded through the transmit optics and sent through space to the receive aperture of the other spacecraft. The fast steering mirrors serve to enhance the pointing acquisition and control of the system and account for internal optical component misalignments.

The received communications signal is resized by the main beam expander/reducer assembly and is reflected off of a fast steering mirror. The signal then passes through the dichroic filter and is split by the beam splitter so that some of the signal hits the Avalanche Photodiode Detector (APD). This detector measures the amount of light hitting it so that the received pulses of light can be demodulated and received.

The transmitted beacon signal is generated by a 976 nm beacon laser diode, set to the proper divergence angle, and sent through free space to the other satellite. The transmitted beacon signal does not pass through the main optical path and is completely separate from the rest of the system.

Part of the received beacon signal passes through a receive lens that is separate from the main beam expander/reducer assembly and is focused onto a silicon camera detector. The beacon location on this camera corresponds to a pointing offset angle that is used for closed-loop control of the reaction wheels for coarse pointing. Another part of the received beacon signal passes through the main beam reducer assembly and is reflected off of the second FSM. The received beacon signal is then reflected off of the dichroic filter and focused onto a Quadrant Cell (quad cell) photodetector. This sensor measures the center location of the beam very accurately, which corresponds to a fine-pointing angular offset that is used for closed-loop control of the second FSM for fine pointing.

The internal calibration signal is a 635 nm beam used in an initial calibration step to measure the alignment of the first FSM in order to compare the angles of the outgoing communications transmit signal and incoming communications and beacon receive signals to ensure that the satellites can point at each other with sufficient accuracy. The calibration beam is collimated by the same collimator as the transmit communications signal. The calibration beam then reflects off of the first FSM, passes through the beam splitter, and is both reflected off of and transmitted through the dichroic filter. The portion of the beam that reflected off of the dichroic reflects off of the flat mirror and is transmitted through the dichroic and focused onto the quadrant cell detector to measure the alignment of the first FSM. This initialization step makes the system more robust and reduces the risk of misalignments from launch/deployment.

Concept of Operations

The concept of operations for the optical crosslinks begins with each satellite receiving information of the other satellite's GPS and orbital location through low-rate radio communications from the ground. The

satellites then use their knowledge of their own orientation from their star tracker sensors to command their reaction wheels and point the lasercom terminals towards each other. At this stage, the satellite body pointing accuracy is expected to be between 100-1200 arcsec. The satellites will then turn on the beacon signals. The beacons have large divergences (1.2 degree half power beam width) in order to account for the pointing uncertainty and mounting misalignments. The satellites will image their received beacon signals on their silicon detectors and use this knowledge to improve the coarse pointing control and keep the satellites directed towards each other. This feedback will improve the body pointing to <360 arcsec.

At this point, the internal calibration beam will be turned on and measured on the quad cell detector. FSM 2 will use the measurement from the quad cell detector to control the mirror and direct the calibration signal to the center of the quad cell detector. This position of the calibration beam will be measured and the calibration beam will be turned off and FSM 2 will be locked in place. The beacon signal will then be pointed accurately enough from the closed-loop body pointing control with feedback from the beacon camera receiver to be measured on the quad cell detector and used for closed-loop control of FSM 1. FSM 1 will use the quad cell position measurement of the incoming beacon signal to steer the beacon signal to the center of the quad cell detector. This will ensure that the incoming receive signal will be aligned properly with the outgoing transmit signal so that the communications link can be achieved. The communications signal strength on the APD will then be used to control FSM 1 until the signal strength on the APD is maximized. The location of the beacon signal on the quad cell detector at this point will be measured and this will be defined as the optimal center beam location. Both satellites will use the quad cell measurements of the beacon signals for closed-loop fine-pointing control to keep the communications signal directed towards the receiver. The system design has the potential for full-duplex operations, but this is not a primary mission requirement.

DESIGN VERIFICATION

Link Budget Analysis

This design has been verified by calculating link budgets for the communications link, the beacon signal to the coarse pointing beacon camera link, and the beacon signal to the quad cell fine pointing link. The results of these calculations are summarized in Figure 3.

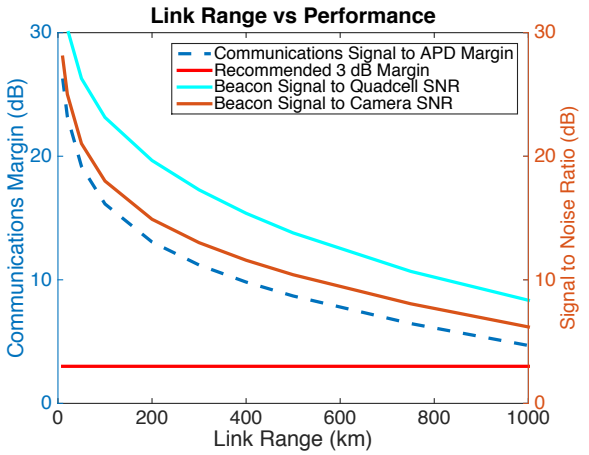

Figure 3: Summary of link calculations for the FLARE optical design over a range of link distances at 20 Mbps data rate. Image credit: Rachel Morgan.

The communications link budget is based on Q-factor analysis for required power as outlined in Ryan Kingsbury's thesis 6. This analysis is based on the assumptions that the system operates at high photon flux and that light intensity in each slot follows a Gaussian distribution. The calculations use the noise equivalent power reported in the specifications sheet for the baseline APD selection (Hamamatsu InGaAs APD G-8931 20) to determine the signal power required for a specified bit error rate (assumed to be 10^{-4} which can be handled with coding). The actual power received is calculated from the transmitter output power and transmitter and receiver gains from the telescope aperture size, accounting for the free space path loss due to the beam divergence, pointing loss based on the assumption that the pointing system will be able to keep the pointing accurate to within the half power beam width, and optics loss estimated from the transmissivity of each optic component. The results of this analysis for a 20 Mbps data rate across the mission link distances are reported in Table 1.

Table 1: Link budget parameters for communications link

Range (km)	20	100	500
Transmit optical power (mW)	200	200	200
Transmit wavelength (nm)	1550	1550	1550
Half power beam width (mrad)	.071	.071	.071
Optics loss (dB)	6.49	6.49	6.49
Pointing loss (dB)	3	3	3
Free space path loss (dB)	224	238	252
Telescope diameter (m)	.02	.02	.02
Data rate (Mbps)	20	20	20
Margin (dB)	23.21	16.14	8.69

The beacon signal to the silicon beacon camera link budget was modeled using the method outlined in Tam Nguyen's thesis on laser beacon tracking for earth to space beacon links 7. This method was adapted for crosslinks by neglecting the atmospheric turbulence losses and changing the noise terms associated with earth's irradiance to represent expected noise from background stars. A conservative value for background optical noise due to stars was calculated from finding the worst-case stellar irradiance at the beacon wavelength from historical data. For a 976 nm beacon signal, the greatest stellar irradiance occurs for only 7 very bright M-class stars which irradiate ~10^{-12} W/cm^2/um^2 8. This irradiance value was assumed for a worst-case link estimate and converted to a photon noise count, which was used in the SNR calculation.

The link budget method calculates the power received on the detector from the transmitter power and transmitter and receiver gains, accounting for the free space path loss due to the beam divergence, pointing loss assuming the pointing is accurate to within the half power beam width, and optics loss estimated from the optical component's transmissivity specifications. It also simulates the image received by the detector to calculate the signal to noise ratio of the link. The image is simulated by generating a Point-Spread-Function (PSF) image for the received beacon optical power and overlaying it on a background frame constructed pixel-by-pixel from background radiance, shot, and detector noise statistics. The signal to noise ratio is calculated by comparing the photoelectron count received from the beacon to the electron counts from the modeled noise sources for the baselined camera selected (mvBlueFox-IGC205 with the Aptina MT9P031 sensor). The results of this analysis for a range of link distances is reported in Table 2. Simulated PSF images for a range of link distances are shown in Figure 4.

Table 2: Link budget parameters for beacon to camera link

Range (km)	20	100	500
Beacon optical power (mW)	500	500	500
Beacon wavelength (nm)	976	976	976
Pointing loss (dB)	3	3	3
Half power beam width (rad)	.021	.021	.021
Free space path loss (dB)	228	242	256
Optics loss (dB)	.2	.2	.2
Receive aperture diameter (m)	.025	.025	.025
Camera quantum efficiency (at 976 nm)	.02	.02	.02
Signal to noise ratio (dB)	25.01	17.99	10.41

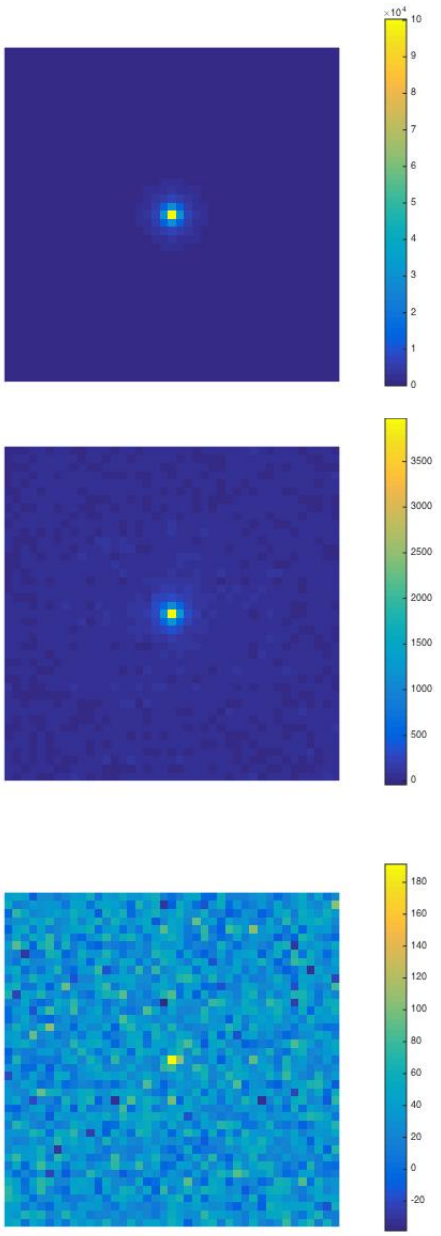

Figure 4: Simulated PSF image on beacon camera for (from top) 20, 100, and 500 km link ranges. Colorbars display electron counts.

The beacon signal to Quadrant Cell (quad cell) photodetector link budget uses the beacon transmitter power, wavelength, and divergence angle and receiver size to calculate the photon flux at the detector. This is converted to a signal electron count through the quantum efficiency of the detector and the integration time of the system. Stellar noise electron counts are

calculated from a worst-case stellar irradiance calculation similar to the beacon signal to camera link. Dark noise electron counts are calculated from the dark current given in the detector specification sheet for the baseline detector selected (Hamamatsu S5980). These electron counts are used to calculate the signal to noise ratio for the beacon signal to quad cell link. The results of these calculations are reported in Table 3.

Table 3: Link budget parameters for beacon to quadcell link

Range (km)	20	100	500
Beacon optical power (mW)	500	500	500
Beacon wavelength (nm)	976	976	976
Pointing loss (dB)	3	3	3
Half power beam width (rad)	.021	.021	.021
Free space path loss (dB)	228	242	256
Optics loss (dB)	4.25	4.25	4.25
Receive aperture diameter (m)	.02	.02	.02
Sensor responsivity (at 976 nm)	.7	.7	.7
Signal to noise ratio (dB)	30.31	23.14	13.78

The FLARE mission will be a technology demonstration for this optical transceiver design and show that the system can operate in space. For future missions, this design can be scaled up to accommodate more challenging mission scenarios. One of the key use cases for communications crosslinks between small satellites is a global constellation of earth observing or communication relay satellites. Global coverage of a satellite constellation requires crosslink ranges of 1,000-7,500 km depending on the density of the constellation satellites 5. The current design can be scaled up to meet these more challenging link requirements by decreasing the data rate, increasing the beacon signal power, and decreasing the beacon signal divergence. Figure 5 shows the link margins for the beacon and communications links for the links with the scaled up design, increasing the beacon power to 2 W, decreasing the beacon beamwidth to .011 rad (a narrower beacon beam implies improved coarse pointing capability and optical alignments), increasing the Lens 1 main aperture diameter to 4 cm, and using a data rate of 5 Mbps. FLARE is using deployable solar panels for differential drag orbit control, which makes longer crosslinks infeasible for the FLARE demonstration mission. Therefore, scaling up the FLARE optical design to enable these longer crosslinks would also require incorporating an on-board propulsion system.

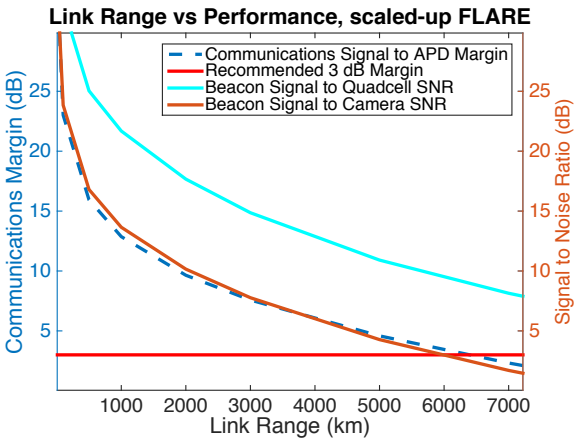

Figure 5: Summary of link calculations for the scaled up version of the FLARE optical design over a range of link distances representative of link ranges required for a global constellation of small satellites. The scaled up version increases the beacon power to 2 W, decreases the beacon beamwidth to .011 rad (a narrower beacon beam implies improved coarse pointing capability), increases the Lens 1 main aperture diameter to 4 cm, and assumes a data rate of 5 Mbps. Image credit: Rachel Morgan

Benchtop Optical Prototype

A bench-top optical transceiver prototype has been developed in lab to demonstrate the system design and start testing its operation. The prototype consists of a transmitter model setup and a transceiver model setup on separate optical breadboards so they are portable and can be tested at different separations. The prototype uses different wavelengths and electronics than will be used in the actual system to keep the cost of the system down and take advantage of easily acquired COTS components. The transmitter model setup transmits a 1550 nm communications signal and a 635 nm beacon signal. The transceiver model receives these signals and transmits at the same wavelength. Since the goal of the prototype system is to demonstrate the overall system architecture, transmitting and receiving at different the actual FLARE wavelengths is not required. The wavelength division in the actual FLARE system enables full duplex operations and ensures that the transmitting communications signal can be filtered so that it cannot reach the receiver as it is being transmitted which reduces noise on the receiver. Demonstrating full-duplex operations is not a goal of this initial prototype.

The transmitter model is a 2-in collimator setup consisting of a two laser fiber sources, an optical fiber mount adaptor, lens tubes, and a 2-in lens to produce a 2-in diameter gaussian beam. The two laser sources

produce light at 1550 nm to demonstrate the communications link and 635 nm to demonstrate beacon acquisition. In the future, a wavelength division multiplexing coupler will be used to combine the two signals to demonstrate simultaneous operations. Both fibers are mounted to the optical fiber mount adaptor and the signals are sent through the lens tube assembly to produce a wide, collimated beam which simulates the other satellite's transmitted communications and beacon signals so the transceiver model can receive them. The transmitter model is pictured in Figure 6. The laser setup is pictured in Figure 7.

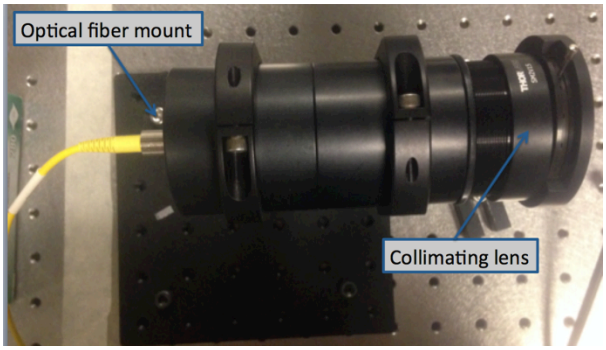

Figure 6: Transmitter setup for FLARE prototype. This setup produces a wide, collimated beam to simulate the signal received by the FLARE transceiver prototype. Image credit: Rachel Morgan.

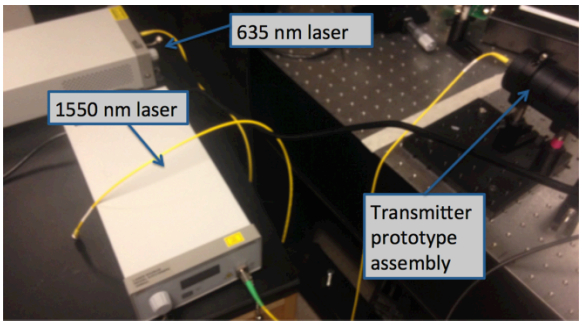

Figure 7: Transmitter setup for FLARE prototype. This setup produces a wide, collimated beam to simulate the signal received by the FLARE transceiver prototype. Image credit: Rachel Morgan.

The transceiver model consists of a beam reducer/expander assembly, a mirror, a dichroic filter, a beam splitter, a visible wavelength quad cell photodetector, and an infrared wavelength APD. The beam reducer/expander assembly consists of two lenses mounted to a lens tube system. The received 1550 nm beam is resized by the beam reducer and reflects off of a mirror. The beam then passes through a dichroic filter and is split by a beam splitter so half of it is sent through a focusing lens onto an IR APD and half of it is dumped. The received 635 nm beacon signal is resized by the beam reducer assembly and reflected off of the mirror. This signal is then reflected off of the dichroic and sent through a focusing lens onto a visible quad cell detector. The quad cell detector will be used for closed-loop feedback control of the fast steering mirror. This setup can also be used to demonstrate transmit operations by adding a second mirror and collimator where the target is pictured. The transceiver model is pictured in Figure 8.

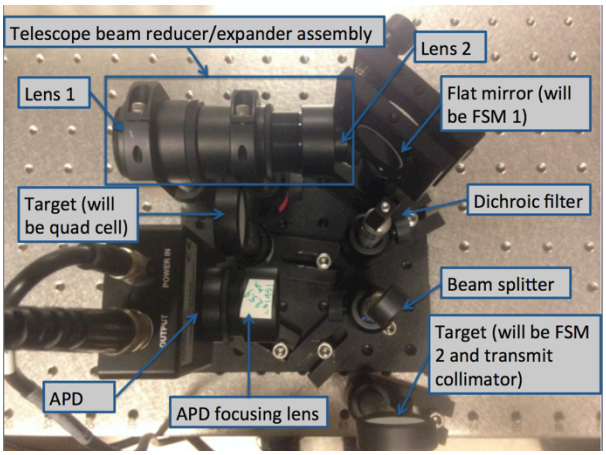

Figure 8: Transceiver setup for FLARE prototype. This setup has been used to demonstrate the communications link and will be modified to conduct tests of the beacon receive and pointing control systems as well as the calibration beam and transmit operation. Image credit: Rachel Morgan.

The bench-top prototype has been used successfully for a hallway demonstration of the system. The transmitter has been used to send a mechanically modulated signal to the transceiver, and the signal has been measured from the receiver APD using an oscilloscope. A picture of this demonstration is shown in Figure 9. The prototype has also demonstrated the beacon receive optics by sending a 635 nm signal and generating a spot on a target where the quad cell detector will be as shown in Figure 10. The prototype will also be used to demonstrate the feedback control system of the FSM using the quad cell in the future. The next step will be to incorporate a calibration beam and a second FSM in the system to demonstrate the full system concept of operations.

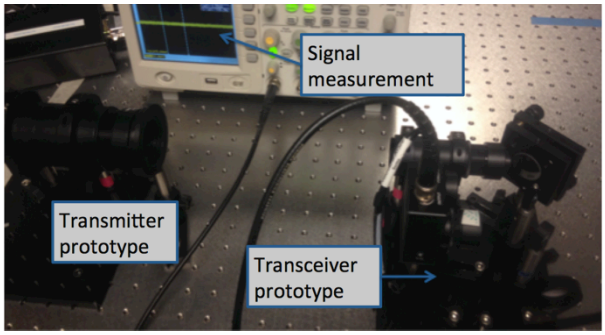

Figure 9: Communications link demonstration with FLARE prototype. A 1550 nm signal was sent by the transmitter prototype and received by the transceiver prototype. The signal was measured from the APD using an oscilloscope. Image credit: Rachel Morgan.

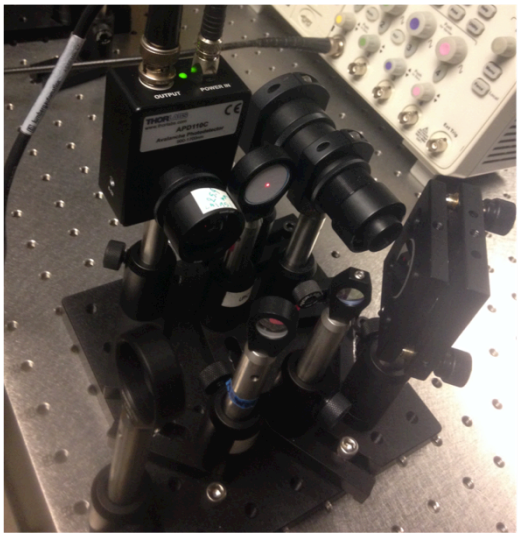

Figure 10: Beacon link demonstration with FLARE prototype. A 635 nm signal was sent by the transmitter prototype and received on a target, which will be replaced by a quad cell detector for closed-loop feedback control of FSM 1. Image credit: Rachel Morgan.

CONCLUSIONS

The FLARE optical communications transceiver has been designed, analyzed, and prototyped for a mission that will demonstrate novel optical communications crosslink capabilities for small satellites. The mission will use a 200 mW modulated optical transmit signal to communicate at 5-20 Mbps at separation distances ranging from 20 km to 500 km. The design has been verified through link budget analysis and preliminary prototyping and testing. The link budget analysis shows that the current design can achieve communications links to meet the FLARE mission requirements with adequate margins.

The prototype has been used for a successful hallway demonstration of the communications link by transmitting a characteristic signal and receiving it through the optical system and measuring it from the APD. It has also been used to demonstrate the beacon signal link by transmitting a visible beacon signal and focusing it on a target. The setup will be used to implement a feedback loop with the APD and FSM 1 to find the optimal beacon location based on the maximum power measured on the APD. It will also be used to demonstrate and test the beacon receive and pointing control systems by implementing closed-loop feedback control of the FSM based on the quad cell measurements. This will involve adding external disturbances to the incoming beacon/communications signals in order to test the ability of the pointing control system to correct for them and keep the communications signal focused on the APD. The next step is to add in a second fast steering mirror and a calibration beam and test the full concept of operations. The prototype will also be updated with actual system components as they are finalized for more realistic component testing and fit-checks of the system.

The FLARE mission will serve to demonstrate the transceiver design and operation in space at limited link ranges. The design is scalable to meet more challenging requirements such as longer link ranges to enable global coverage in a constellation. Link budgets have been calculated to show what upgrades to the system would be necessary to achieve link ranges of 1000-7000 km for use in a global constellation of small satellites.

Acknowledgments

The author would like to thank Prof. Kerri Cahoy and graduate students Michael Long and Hyosang Yoon for their help and mentorship. The author would also like to acknowledge the MIT SuperUROP program for their funding and support.

References

1. Clements, E. and R. Aniceto et al., “Nanosatellite Optical Downlink Experiment: Design, Simulation, and Prototyping,” Optical Engineering, vol. 55, No. 1, November 2016.
2. Janson, S. and R. Welle, “The NASA Optical Communication and Sensor Demonstration Program,” Proceedings of the 27th Annnual AIAA/USU Conference on Small Satellites, Logan, UT, August 2013.
3. Gregory, M. and F. Heine et al., “TESAT Laser Communication Terminal Performance Results

on 5.6 Gbit Coherent Inter Satellite and Satellite to Ground Links," Proceedings of the International Conference on Space Optics ISCO, 2010.

4. Nag, S., "Design and Analysis of Distributed Nano-Satellite Systems for Multi-Angular, Multi-Spectral Earth Observation," Proceedings of the 64th International Astronautical Congress, 2013.

5. Shuber, P. and A. Cline et al., "System Design of Low SWaP Optical Terminals for Free Space Optical Communications," Proceedings of SPIE, vol. 10096, 2017.

6. Kingsbury, R., "Optical Communications for Small Satellites," PhD Dissertation, Massachusetts Institute of Technology, Cambridge, MA, 2015.

7. Nyugen, T., "Laser Beacon Tracking for Free-Space Optical Communication on Small-Satellite Platforms in Low-Earth Orbit," Master's thesis, Massachusetts Institute of Technology, Cambridge, MA, 2015.

8. Ramsey, P. C., "Spectral Irradiance from Stars and Planets, Above the Atmosphere, from .1 to 100.0 Microns," Applied Optics, vol. 1, issue 4, 1962.